ORIGINAL ARTICLE

Validated High-Resolution Melting Assays for Efficient Screening of *DENND1A, LHCGR, FSHR, THADA,* and *CYP17A1* Polycystic Ovary Syndrome-Associated Gene Polymorphisms

Mariam Elbadie[1,3], Habibah Abdul Hamid[2], Zalinah Ahmad[4,5] , King-Hwa Ling[1,3]

[1] Department of Biomedical Science, Faculty of Medicine and Health Sciences, University Putra Malaysia, 43400 UPM, Serdang, Selangor, Malaysia
[2] Department of Obstetrics & Gynaecology, Faculty of Medicine and Health Sciences, University Putra Malaysia, 43400 UPM, Serdang, Selangor, Malaysia
[3] Genetics and Regenerative Medicine Research Centre, Faculty of Medicine and Health Sciences, University Putra Malaysia, 43400 UPM, Serdang, Selangor, Malaysia
[4] Department of Pathology, Faculty of Medicine and Health Sciences, Universiti Putra Malaysia, 43400 UPM, Serdang, Selangor, Malaysia
[5] Laboratory of Vaccine and Biomolecules (VacBio), Institute of Bioscience, Universiti Putra Malaysia, 43400 UPM, Serdang, Selangor, Malaysia

ABSTRACT

Introduction: High-resolution melting (HRM) analysis is a fast, sensitive, cost-effective, post-qPCR mutation detection method. HRM analysis represents an advancement over previous DNA dissociation studies, serving to classify DNA samples based on their dissociation behaviour as they melt from dsDNA to ssDNA, utilising special dsDNA saturating fluorescent dyes such as LCGREEN, EVaGreen, and ResoLight. This study aimed to design and validate high-resolution melting assays for the screening of six polycystic ovary syndrome (PCOS) associated single-nucleotide polymorphisms, namely *DENND1A* (DENN/MADD domain-containing 1A) rs2479106 and rs10986105, *THADA* (Thyroid Adenoma-Associated Protein) rs13429458, *LHCGR* (Luteinising Hormone/Choriogonadotropin Receptor) rs13405728, *FSHR* (Follicle-Stimulating Hormone Receptor) rs6166, and *CYP17A1* (Cytochrome P450 17A1) rs743572. **Materials and methods:** A total of forty-five peripheral blood samples obtained from the infertility clinic at Hospital Sultan Abdul Aziz Shah were collected for gDNA extraction, primers were designed, and optimised for HRM analysis to be conducted on the Light cycler release 1.5.1.62SP3 software. **Results:** The HRM-predicted genotypes of these target SNPs in all gDNA samples were 100% consistent with Sanger DNA sequencing results, illustrating the accuracy and efficiency of this method for high-throughput SNP genotyping. **Conclusion:** HRM is an efficient technique for rapidly and effectively screening specific SNPs across a large-scale population study.
Malaysian Journal of Medicine and Health Sciences (2025) 21(6): 1-9. doi:10.47836/mjmhs.v21.i6.945

Keywords: Genotype, SNPs, Polycystic ovary syndrome, Sequencing analysis, Mutation

Corresponding Author:
King-Hwa Ling, PhD
Email: lkh@upm.edu.my
Tel : +60397692564

INTRODUCTION

Polycystic ovary syndrome (PCOS) is the most prevalent endocrinopathy in reproductive-aged women and a significant contributor to anovulatory infertility, with a prevalence of 5-10% [1], while it was counted to affect 12.6% of the Malaysian population [2]. Although the exact cause of PCOS remains incompletely elucidated, multiple environmental, genetic, and metabolic factors are involved in its pathogenesis [3] . Early studies demonstrated that PCOS-related traits were more prevalent in the siblings of affected women, suggesting a model of autosomal dominant inheritance. However, twin studies have since revealed PCOS to be a polygenic or X-linked disorder [4]. Furthermore, twin studies have estimated that genetic factors account for 72% of the variance in PCOS risk, underscoring the significant genetic contribution [5] . The first genome-wide association study conducted in the Chinese population identified three PCOS susceptibility loci, corresponding to the *LHCGR*, *THADA*, and *DENND1A* genes located at 2p16.3, 2p21, and 9q33.3, respectively [6]. A subsequent, expanded GWAS in Han Chinese individuals identified eight risk loci. In total, these two-stage GWAS studies have uncovered 11 genetic risk regions near or within candidate genes associated with PCOS [7] .

Connecdenn 1/2 are proteins containing DENN

(differentially expressed in normal and neoplastic cells) domains, which act as guanine nucleotide exchange factors for the small GTPase Rab35. When connecdenn/Rab35 function is disturbed, it results in abnormalities in the recycling of various cargo proteins from endosomes, leading to changes in cell function [8]. Immunohistochemical analyses demonstrated that *DENND1A*.V2 was higher in PCOS theca cells than in normal theca cells [9]. The *DENND1A* gene displays a variety of genetic variations, such as rs10818854, rs2479106, and rs10986105 (intronic variants), that have been linked to PCOS in Han Chinese women and other ethnicities [10–12].

The luteinising hormone/chorionic gonadotropin receptor (*LHCGR*) is a member of the G protein-coupled receptor superfamily and other glycoprotein hormone receptors. It is the targeted receptor for both the luteinising hormone (LH) and placental chorionic gonadotropin (CG) [3]. A recent GWAS research study has linked the 2p16.3 region containing *LHCGR* loci with PCOS among Han Chinese and European populations [13]. Specifically, the intronic variant rs13405728 within the *LHCGR* gene showed an association with PCOS in Han Chinese women [14]. The human *FSHR* (follicle-stimulating hormone receptor) is a G protein-coupled receptor with a long extracellular domain consisting of 7 transmembrane regions, 3 short intracellular loops, 3 additional loops, and an intracellular tail. It binds to FSH using its large ECD (extracellular domain) [15]. Numerous studies have thoroughly examined the relationship between *FSHR* gene polymorphisms, Thr307Ala (rs6165) or Asn680Ser (rs6166) coding sequence changes, and PCOS, yielding varying and disputed findings [16].

The thyroid adenoma-associated protein (*THADA*), linked to thyroid adenoma, is found in various organs, including the pancreas. The *THADA* gene has been linked to the death receptor pathway and apoptosis [17]. The relationship between the *THADA* gene and PCOS has been demonstrated by associations between *THADA* SNPs and type 2 diabetes [6] The enzyme 17-α-hydroxylase/17–20 lyase (P450 17α) serves as a key regulator in androgen synthesis by facilitating the conversion of pregnenolone to 17-hydroxy-pregnenolone and progesterone to 17-hydroxyprogesterone (17-OHP), which is a rate-limiting step. CYP17 is primarily found in the adrenal gland, testicular Leydig, and ovarian theca cells. It has been suggested that increased activity of this enzyme may lead to heightened synthesis and release of androgens in PCOS [18]. The *CYP17A1* gene variants have been associated with activating the CYP17 promoter or affecting its mRNA in theca cells among those with PCOS [19].

In 1997, Ririe et al. were the first to introduce melting analysis as an extension of real-time PCR reaction monitoring [20]. The combination of PCR product melting analysis with real-time PCR became possible with the LightCycler technology [21,22]. The ability of double-stranded DNA (dsDNA) fragments to denature with increasing temperature, in the presence of an intercalating dye, can be monitored as a sigmoidal-shaped melting curve that reflects the gradual loss of fluorescence. The melting temperature (Tm) is primarily determined by the GC content (%G+C) of the amplicon [23]. The first attempts to detect changes in PCR products through melting curve analysis and to screen for heterozygosity were performed using SYBR Green I dye (for amplicons up to 167 bp) [24]. However, this approach required prior amplicon purification and the addition of extra dye [24] or urea [25]. To overcome these limitations, specialised saturating dyes were developed that could be used at higher concentrations without inhibiting PCR [24,26]. The development of LCGreen dye led to the initial implementation of high-resolution melting analysis (HRMA) in laboratories [21], followed by advancements in instrumentation, software, and fluorescent dye chemistry [22].

High-resolution melting is effectively used for detecting most single-nucleotide variants (SNPs) and the majority of small deletions or insertions [27]. In the presence of SNP, different genotypes exhibit distinctly different melting curve behaviours, together with other sequence characteristics of the amplicon (primarily the GC content and the length) [28].

Despite the association of these genetic variants with PCOS across diverse populations, a significant challenge remains in implementing rapid and cost-effective screening approaches. Current genotyping methods, such as PCR-RFLP (Restriction Fragment Length Polymorphism), Allele-specific PCR, TaqMan PCR, and other multiplex genotyping assays, are often time-consuming, expensive, or complex, which limits their widespread implementation [29]. Our study aimed to develop and validate high-resolution melting assays that can accurately, quickly, and cost-effectively screen for key PCOS-associated gene variants, including *DENND1A* rs2479106 and rs10986105, *THADA* rs13429458, *LHCGR* rs13405728, *FSHR* rs6166, and *CYP17A1* rs743572.

MATERIALS AND METHODS

Obtaining samples and ethical approval

The Medical Research and Ethics Committee, Ministry of Health Malaysia, granted ethical approval (NMRR-18-3175-44106) for the study involving human subjects. Written consent was obtained from participants, and genomic DNA was extracted from the blood samples of forty-five consenting individuals.

Genomic DNA preparation

Genomic DNA was extracted from anticoagulated whole blood samples using the QIAamp® DNA Mini

Kit (QIAGEN, Germany), following the manufacturer's protocol. The quality of the extracted DNA was evaluated with a Lambda PCRmax UV spectrophotometer, and only samples with an A260/A280 absorbance ratio between 1.7 and 1.9 were deemed to be of high purity. The DNA samples were then subjected to electrophoresis on a 1% agarose gel for 40 minutes at 100 volts. After staining with VIsafe red gel stain, the bands were visualised using the BOX BioImaging System. Gel images were captured using GeneSnap software. All extracted genomic DNA samples were stored at -20°C for future use.

Primer design and optimisation through gradient PCR

All Primer sequences shown in (Table I) were designed using the Primer3 web-based tool [30] and subsequently ordered from Integrated DNA Technologies, Singapore. A temperature range of 55-65 °C was set using the MasterCycler Gradient Thermal Cycler machine (Eppendorf) for primers optimisation to determine the optimal annealing temperature. PCR amplicons were then electrophoresed using a 2% (w/v) agarose gel for 40 minutes at 120V.

Table I: The properties of the designed primers for high-resolution melting assays

Gene	Variant	Alleles	Forward / Reverse primers	Tm (°C)	Amplicon (bp)	GC%
DENND1A	rs2479106	A/G	F: GAGCAGCCACTCAAGAAACAG R: GCAGCTTAATGTGATGCCACT	60.19 60.29	166	52.38 47.62
DENND1A	rs10986105	T/G	F: CCAATTTCCATCACAATTAGCC R: GGTGCCCTTTCTCTTAAGGTTT	60.55 60	151	40.91 45.45
THADA	rs13429458	A/C	F: GAATGCACAATGGAGACTGCT R: TGTACCGTGCTTCTGAACAAA	60.28 59.38	149	47.62 42.86
LHCGR	rs13405728	A/G	F: AGGGATGCTGGAAAACATTCT R: CTCACCATAATGCAGCCATTT	59.95 59.97	152	42.86 42.86
FSHR	rs6166	C/T	F: TACCCTTCAAAGGCAAGACTG R: CTCTTCAGCTCCCAGAGTCAC	59.36 59.19	134	47.62 57.14
CYP17A1	rs743572	A/G	F: ACCTTCTCTTGGGCCAAAACA R: CCTCCTTGTGCCCTAGAGTTG	60.06 60.07	139	47.62 57.14

* *DENND1A*: DENN/MADD domain-containing 1A; *THADA*:Thyroid Adenoma-Associated Protein; *LHCGR*: Luteinising Hormone/Choriogonadotropin Receptor; *FSHR*:Follicle-Stimulating Hormone Receptor; *CYP17A1* Cytochrome P450 17A1; Tm: Melting Temperature; bp: Base Pair; GC%: Guanine and Cytosine Percentage.

qPCR efficiency and HRMA

Four serially diluted reactions with a 1/2 dilution factor were prepared in triplicate on a LightCycler 480 Multiwell Plate 96 from Roche, along with a negative control (non-template control), to evaluate the qPCR efficiency. gDNA samples were diluted to fit the recommended concentration range of the LightCycler® 480 High-Resolution Melting Master that contains a special saturating fluorescent dye (LightCycler® 480 ResoLight Dye). The 20µl HRM-reaction mixture consisted of 10 µl (1X) LightCycler® 480 High-Resolution Melting Master (Roche), 1 µl (5- 30ng/dl) of genomic DNA, 1 µl (4µM) primer mix, 2 µl (2.5 mM) MgCl2, and PCR-grade water for the final reaction volume adjustment. The amplification was carried out using LightCycler® 480 System (Roche), with the following cycle condition: initial denaturation at 95 °C for 10 min, followed by 45 cycles of amplification at 95 °C for 10s, annealing at 55 °C (for all six sets of primers) for 15s, and a final extension at 72 °C for 10s.

Amplicons were then subjected to high-resolution melting (HRM) analysis on the same machine, beginning with a melting curve protocol consisting of 95 °C for 1 minute, 40 °C for 1 minute, 65 °C for 1 second, and 95 °C with 25 acquisitions per 1 °C increment, followed by cooling at 40 °C for 10 seconds. The Light Cycler® release 1.5.1.62SP3 software was utilised to monitor the real-time amplification and analyse the melting characteristics. The gene scanning module generates the normalised melting curves and the temperature-shifted differential plots that categorise the genotypes for each sample based on their melting profiles.

Sequencing

One representative sample from each melting curve was selected following HRM analysis and purified using a Primeway Gel extraction/PCR purification kit (First BASE Laboratories Sdn. Bhd., Malaysia) following the manufacturer's instructions, the concentration of the purified amplification products was measured using the Lambda PCRmax NanoDrop spectrophotometer before sending them for sanger sequencing through the services offered by First BASE Laboratories Sdn. Bhd., Malaysia. Sequencing results were viewed using Unipro UGENE software [31], and subsequently compared to the reference sequences obtained from the National Center for Biotechnology Information (NCBI).

RESULTS

Samples and qPCR optimisation

The DNA samples had a mean A260/280 absorbance ratio of 1.7±0.06. Subsequently, the samples underwent electrophoresis on a 1% (w/v) agarose gel to assess their integrity (Fig. 1). All bands were observed above the 10 kb marker and appeared intact, with light smearing, indicating that the samples possessed high genomic DNA integrity. Gradient PCR was employed to ascertain the specificity of the primers for *DENND1A*

gene variants rs2479106 and rs10986105, *THADA* gene variant rs13429458, *LHCGR* gene variant rs13405728, *FSHR* gene variant rs6166, and *CYP17A1* gene variant rs743572 at various temperatures. The optimal annealing temperature was established using gel electrophoresis, which displayed a distinct and bright band indicating the presence of the specific product. The primers for *DENND1A* variants exhibited specific binding across all temperatures set (Fig.2 A and B), while the other primers displayed distinct specific bands at lower temperatures. Notably, all primers amplified specific bands at an annealing temperature of 55 °C (Fig. 2 C, D, E, and F); therefore, PCR efficiencies for all assays were evaluated at this temperature. Following the determination of the observed specificity of the annealing temperature. Reaction conditions were optimised, and a standard curve was generated to assess PCR primer efficiency. Efficiency at an annealing temperature of 55°C was calculated using the equation derived from the standard curve (Fig.2), the PCR efficiency was 94.65% (R^2=0.98), 104.9% (R^2 =0.99), 116.5% (R^2 =0.99), 98.4% (R^2 =0.93),104.3% (R^2 =0.99), and 111.5% (R^2=0.99) for rs2479106, rs10986105, rs13405728, rs6166, rs13429458, and rs743572 respectively. A single unique melting peak was obtained from all the prepared samples for all the PCR assays. The HRM assays demonstrated high efficiency in this experimental context.

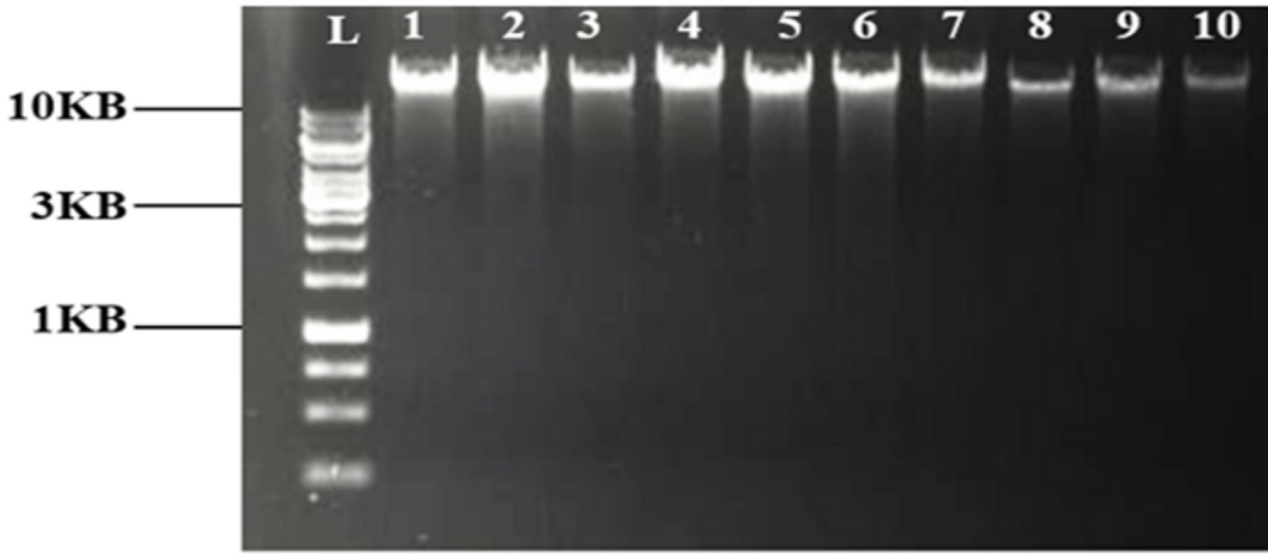

Fig 1: A 1X gel electrophoresis image demonstrates the integrity of the extracted genomic DNA samples. L refers to the 1KB ladder from ThermoScientific™. Lanes 1-10 are representative gDNA samples of good integrity.

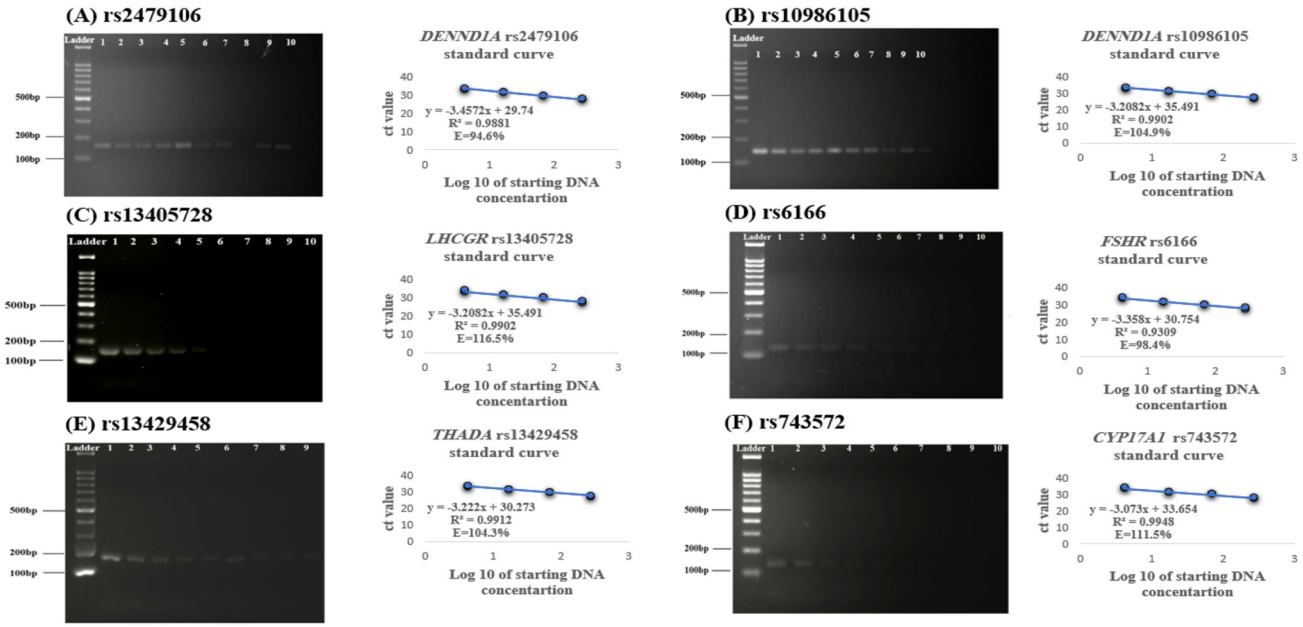

Fig 2. The optimisation of the annealing temperature and the standard curve demonstrating the qPCR efficiency for (A) DENND1A rs2479106 primers (166bp), (B) DENND1A rs10986105 primers (151bp), (C) LHCGR rs13405728 primers (152bp), (D) FSHR rs6166 primers (134bp), (E) THADA rs13429458 primers (149bp), and (F) CYP17A1 rs743572 primers(139bp). The annealing temperature for the primers was set in a temperature range between 55-65 °C (1=55.2, 2=56, 3=57, 4=58.2, 5=59.4, 6=60.6, 7=61.8, 8=63, 9=64, 10=65). The log10 concentration was based on arbitrary units (a.u.). E: Efficiency; R^2 : coefficient of determination.

HRM analysis

Different genotypes exhibit distinct melting curve behaviors when a single-nucleotide polymorphism (SNP) is present. Homozygous allelic variants result in a temperature shift along the X-axis of the high-resolution melting (HRM) curve, while heterozygous variants lead to changes in the curve shape. For heterozygotes, the melting curve comprises both heteroduplex and homoduplex components, shifting left to lower temperatures as they dissociate more readily. HRM analysis revealed three distinctive melting curves for the *DENND1A* rs2479106 variant (Fig. 3A), corresponding to the genotypes: wild-type AA, heterozygous AG, and mutant GG. In contrast, only two melting peaks were observed for the *DENND1A* rs10986105 variant (Fig. 3B), representing the wild-type TT and heterozygous TG genotypes.

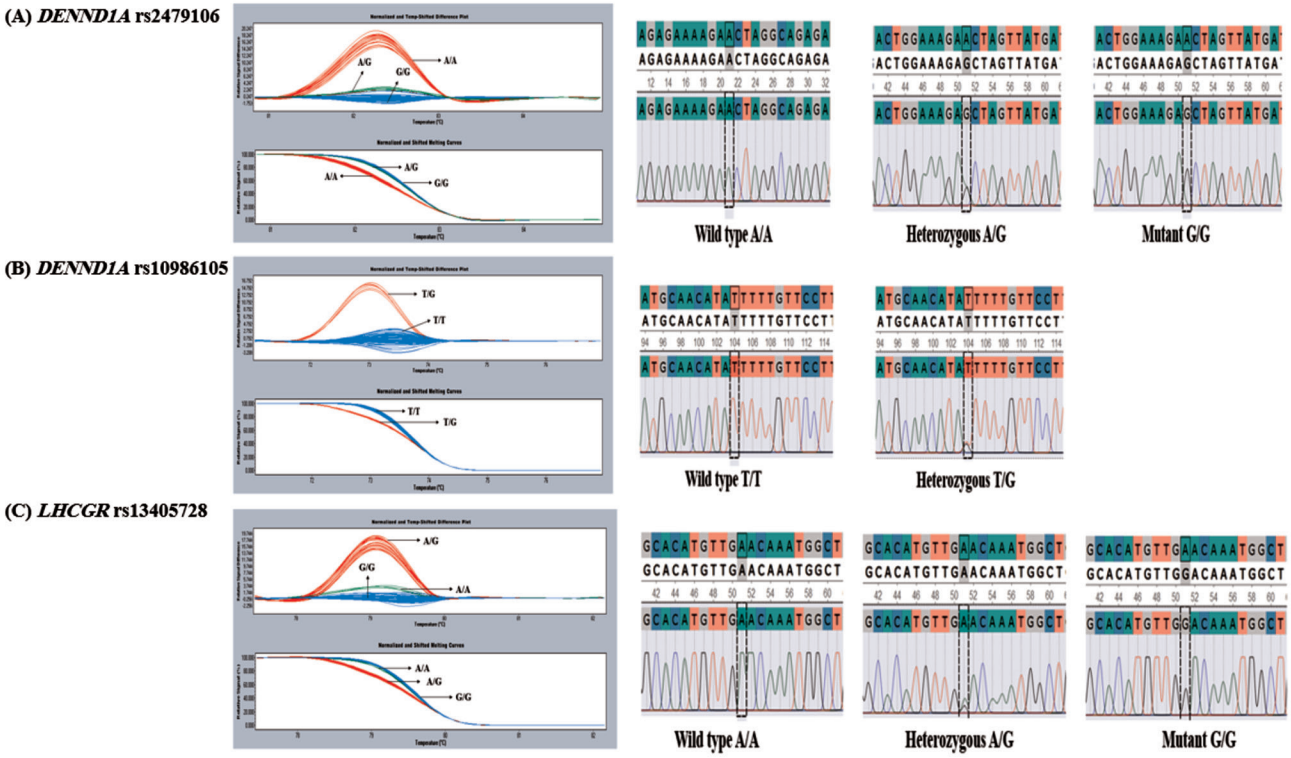

Fig 3: The normalised melting curves and temperature-shifted difference plots are presented, each with the corresponding genotype. The sequencing results are shown in the chromatogram of (A) DENND1A rs2479106, (B) DENND1A rs10986105, and (C) LHCGR rs13405728. A single peak indicates homozygous wild-type or mutant genotypes, while the heterozygous genotype appears with two overlapping peaks of different colours.

The *LHCGR* rs13405728 gene variant demonstrated three melting curves for its three genotypes (Fig. 3C): wild-type AA, heterozygous AG, and mutant GG. Similarly, the *FSHR* rs6166 gene variant displayed three melting peaks (Fig. 4A) corresponding to its three genotypes: wild-type CC, heterozygous CT, and mutant TT. The *THADA* rs13429458 gene variant presented four unique melting curves (Fig. 4B). Among these, two curves represented the wild-type AA and heterozygous AC genotypes, while the additional two curves arose from two adjacent SNPs within the amplicon: rs1317772225 (insertion of C/–) and rs7568365 with two genotypes TT/CT. Moreover, the *CYP17A1* rs743572 gene variant showed two melting peaks (Fig. 4C) for the wild-type genotype AA and the heterozygous genotype AG. The genotyping results are provided in (Table II). Notably, the results from HRM were compared with sequencing results, which matched 100%, confirming the specificity of the assays (Fig. 3 and 4).

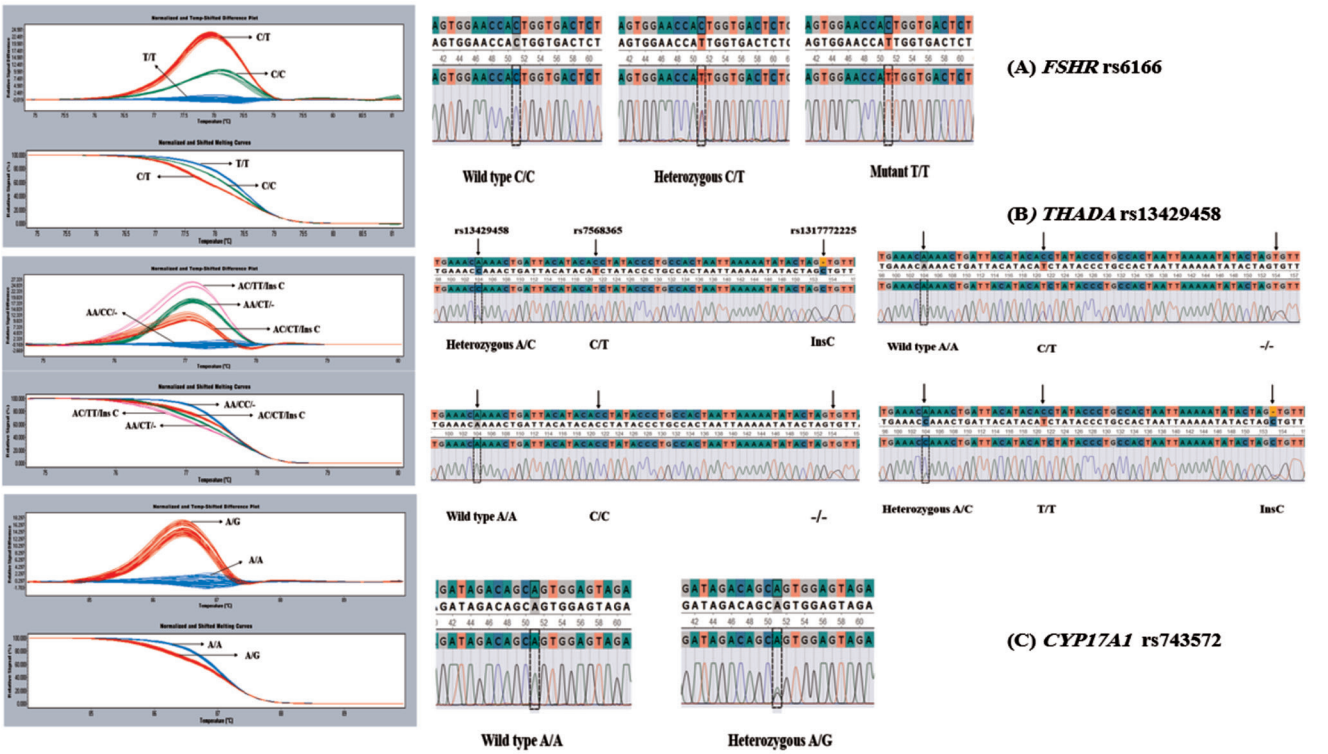

Fig 4: The normalised melting curves and temperature-shifted difference plots are presented, each with the corresponding genotype. The sequencing results are shown in the chromatograms of (A) FSHR rs6166, (B) THADA rs13429458 with the two neighbouring SNPs rs7568365 and rs1317772225, respectively, within the 149 bp amplicon indicated by arrows, and (C) CYP17A1 rs743572. InsC: Insertion of C; the Hyphen represents the absence of C insertion.

Table II: Genotyping Results of the Screened Samples

Gene	Variant	Genotype	N=45
DENND1A	rs2479106	AA	34
		AG	10
		GG	1
DENND1A	rs10986105	TT	44
		TG	1
		GG	0
LHCGR	rs13405728	AA	3
		AG	20
		GG	22
FSHR	rs6166	CC	6
		CT	21
		TT	18
THADA	rs13429458	AA	24
		AC	21
		CC	0
THADA	rs7568365	CC	22
		CT	20
		TT	3
THADA	rs1317772225	-/InsC	17
		-/-	28
CYP17A1	rs743572	AA	21
		AG	24
		GG	0

DISCUSSION

Unlike the conventional mutation scanning techniques that demand a separation step of the PCR products, such as restriction fragment length polymorphism analysis (RFLP) [32], single-strand conformational polymorphism (SSCP) analysis [33], heteroduplex analysis [34], denaturing gradient gel electrophoresis [35], and denaturing high-performance liquid chromatography (DHPLC) [36], high-resolution melting analysis is a closed-tube (decreased contamination risk) SNP genotyping method [37]. On the other hand, more sophisticated methods such as the widely used TaqMan assay, which relies on fluorogenic probes and requires specialised instrumentation, and the conventional Sanger sequencing technique, which remains a standard approach in genotyping, are also commonly employed [38]. Fitarelli-Kiehl et al. compared Sanger sequencing, PCR-RFLP, TaqMan, and high-resolution melting analysis (HRMA) for genotyping the TP53 p.R337H variant, evaluating each method in terms of turnaround time, cost, and accuracy. HRMA was identified as the most cost-effective method (R$18.84 per sample), while Sanger sequencing was the most expensive (R$53.29 per

sample) but also the most robust in terms of accuracy. In terms of speed, TaqMan demonstrated the shortest total and hands-on turnaround time (approximately 3 hours), followed by HRMA (approximately 5.25 hours) [39]. HRMA is a simple and convenient gene scanning method [40–42]. With a special stable fluorescent saturating dye, PCR reagents, followed by post-PCR-melting analysis, the heterozygote scanning sensitivity approaches 100% [22].

The scanning error rate is influenced by the size of the PCR product (amplicon) and the specific type of base alteration, rather than by the SNP's position [37]. The identification of the heterozygotes is based on the change in the shape melting curve [43], while the wild-type and mutant homozygous are distinguished by the change in the melting temperature (Tm). The differences in Tm between genotypes become more noticeable as the size of the amplicon decreases, allowing for better differentiation [32].

In this study, using gDNA samples, HRM assays were established and validated for the detection of *DENND1A* rs2479106 and rs10986105 polymorphisms, *LHCGR* rs13405728, *FSHR* rs6166, *THADA* rs13429458, and *CYP17A1* rs743572 gene variants. For rs2479106, as shown in (Fig.3 A), rs13405728 (Fig.3 C), and rs6166 (Fig.4 A), three distinctive melting profiles appeared, representing the three genotypes of each variant (Homozygous wild-type, Heterozygous, and Homozygous mutant). Meanwhile, only two genotypes were obtained from the melting profiles of rs10986105, wild-type and heterozygous (Fig.3 B), and rs743572, wild-type and heterozygous (Fig.4 C). Four notably unique melting profiles were seen in rs13429458 (Fig.4 B) due to the presence of two additional SNPs within our targeted PCR product, namely, rs7568365 with two genotypes (TT/CT) and an insertion of cytosine polymorphism rs1317772225.

HRM results were confirmed by Sanger sequencing, which demonstrated a 100% correlation with the HRM screening, indicating complete specificity and accuracy of the assays. High-resolution melting analysis is a highly sensitive scanning method that can detect most small deletions or insertions [43]. It has been applied in mutation scanning in genetics, oncology, and bacterial speciation [27]. Many increasing reports on HRM have appeared in the literature, making it a superior and one of the most used methods for future genome analysis [44,45].

However, the high sensitivity of HRMA comes with a price, where certain limitations emerge. In multiple SNP detection, different gDNA extraction methods, variations in the quality and quantity of gDNA, master mix preparation, and pipetting errors can generate faulty, separate clusters in the melting curve analysis [46,47]. While the amplicon length can significantly impact melting curve resolution and sensitivity [48]. The shorter the amplicon, the better-defined the curve. An amplicon size of 150–250 bp is generally optimal for gene scanning [42]. Additionally, variable-number tandem repeats [49], nucleotide transversions (such as A:T and G:C) [50], and small insertions or deletions are difficult to distinguish due to their minimal influence on melting temperature [22].

CONCLUSION

Validated HRM assays were successfully developed for the screening of six SNPs: *DENND1A* rs2479106 and rs10986105 polymorphisms, *LHCGR* rs13405728, *FSHR* rs6166, *THADA* rs13429458, and *CYP17A1* rs743572. The sequencing results showed 100% matching to the HRM findings, making HRM analysis a precise, highly accurate, uncomplicated, rapid, reliable, and cost-effective genotyping method.

ACKNOWLEDGEMENT

The research was funded by Universiti Putra Malaysia, located in 43400, UPM Serdang, Selangor, Malaysia, through a grant from the Geran Putra Berimpak Vote project-UPM/800-3/3/1/GPB/2018/9658500.

REFERENCES

1. Hiam D, Moreno-Asso A, Teede HJ, Laven JSE, Stepto NK, Moran LJ, et al. The genetics of polycystic ovary syndrome: An overview of candidate gene systematic reviews and genome-wide association studies. J Clin Med. 2019;8(10). doi: 10.3390/jcm8101606.
2. Dashti S, Latiff LA, Hamid HA, Saini SM, Bakar ASA, Sabri NAIB, et al. Prevalence of Polycystic Ovary Syndrome among Malaysian Female University Staff. Journal of Midwifery and Reproductive Health. 2019;7:1567–1575. doi: 10.22038/jmrh.2018.30370.1329.
3. De Leo V, Musacchio MC, Cappelli V, Massaro MG, Morgante G, Petraglia F. Genetic, hormonal and metabolic aspects of PCOS: An update. Reproductive Biology and Endocrinology. 2016;14(1). doi: 10.1186/s12958-016-0173-x.
4. Jones MR, Goodarzi MO. Genetic determinants of polycystic ovary syndrome: progress and future directions. Fertil Steril. 2016;106(1):25–32. doi: 10.1016/j.fertnstert.2016.04.040.
5. Khan MJ, Ullah A, Basit S. Genetic basis of polycystic ovary syndrome (PCOS): Current perspectives. Application of Clinical Genetics. 2019;12:249–60. doi: 10.2147/TACG.S200341.
6. Alarcyn-Granados MC, Moreno-Ortнz H, Esteban-Pйrez CI, Ferrebuz-Cardozo A, Camargo-Villalba GE, Forero-Castro M. Assessment of *THADA* gene polymorphisms in a sample of Colombian women with polycystic ovary syndrome: A pilot study.

Heliyon. 2022;8(6). doi: 10.1016/j.heliyon.2022.e09673.
7. Zhao H, Lv Y, Li L, Chen Z-J. Genetic Studies on Polycystic Ovary Syndrome. Best Pract Res Clin Obstet Gynaecol . 2016;37:56–65. doi: 10.1016/j.bpobgyn.2016.04.002
8. Kulasekaran G, Nossova N, Marat AL, Lund I, Cremer C, Ioannou MS, et al. Phosphorylation-dependent regulation of connecdenn/DENND1 guanine nucleotide exchange factors. Journal of Biological Chemistry. 2015;290:17999–8008. doi: 10.1074/jbc.M115.636712.
9. McAllister JM, Legro RS, Modi BP, Strauss JF. Functional genomics of PCOS: from GWAS to molecular mechanisms. Trends in Endocrinology & Metabolism. 2015;26:118–24. doi: 10.1016/J.TEM.2014.12.004.
10. Alizzi FJ, Kokaz HT, Al-Mayah QS. *Dennd1a* and *thada* gene polymorphism among iraqi women with polycystic ovary syndrome. International Journal of Women's Health and Reproduction Sciences. 2020;8:265–71. doi: 10.15296/ijwhr.2020.43.
11. Wan P, Meng L, Huang C, Dai B, Jin Y, Chai L, et al. Replication study and meta-analysis of selected genetic variants and polycystic ovary syndrome susceptibility in Asian population. J Assist Reprod Genet. 2021;38:2781–9. doi: 10.1007/s10815-021-02291-1.
12. Welt CK, Styrkarsdottir U, Ehrmann DA, Thorleifsson G, Arason G, Gudmundsson JA, et al. Variants in *DENND1A* Are Associated with Polycystic Ovary Syndrome in Women of European Ancestry. J Clin Endocrinol Metab. 2012;97(7):E1342–E1347. doi: 10.1210/jc.2011-3478.
13. Hayes MG, Urbanek M, Ehrmann DA, Armstrong LL, Lee JY, Sisk R, et al. Genome-wide association of polycystic ovary syndrome implicates alterations in gonadotropin secretion in European ancestry populations. Nat Commun. 2015;6. doi: 10.1038/ncomms8502.
14. Chaudhary H, Patel J, Jain NK, Joshi R. The role of polymorphism in various potential genes on polycystic ovary syndrome susceptibility and pathogenesis. J Ovarian Res. 2021;14(1). doi: 10.1186/s13048-021-00879-w.
15. Bhartiya D, Patel H. An overview of FSH-*FSHR* biology and explaining the existing conundrums. J Ovarian Res. 2021;14(1). doi: 10.1186/s13048-021-00880-3.
16. Kim JJ, Choi YM, Hong MA, Chae SJ, Hwang K, Yoon SH, et al. FSH receptor gene p. Thr307Ala and p. Asn680Ser polymorphisms are associated with the risk of polycystic ovary syndrome. J Assist Reprod Genet. 2017;34:1087–93. doi: 10.1007/s10815-017-0953-z.
17. Dadachanji R, Sawant D, Patil A, Mukherjee S. Replication study of *THADA* rs13429458 variant with PCOS susceptibility and its related traits in Indian women. Gynecological Endocrinology. 2021;37:716–20. doi: 10.1080/09513590.2021.1906854.
18. Kaur R, Kaur T, Kaur A. Genetic association study from North India to analyze association of CYP19A1 and *CYP17A1* with polycystic ovary syndrome. J Assist Reprod Genet. 2018;35:1123–9. doi: 10.1007/s10815-018-1162-0.
19. Munawar Lone N, Babar S, Sultan S, Malik S, Nazeer K, Riaz S. Association of the CYP17 and CYP19 gene polymorphisms in women with polycystic ovary syndrome from Punjab, Pakistan. Gynecological Endocrinology. 2021;37:456–61. doi: 10.1080/09513590.2020.1822803.
20. Ririe KM, Rasmussen RP, Wittwer CT. Product Differentiation by Analysis of DNA Melting Curves during the Polymerase Chain Reaction. Anal Biochem 1997;245:154–60. doi: 10.1006/abio.1996.9916.
21. Wittwer CT, Reed GH, Gundry CN, Vandersteen JG, Pryor RJ. High-Resolution Genotyping by Amplicon Melting Analysis Using LCGreen. Clin Chem . 2003;49:853–60. doi: 10.1373/49.6.853.
22. Wittwer CT. High-resolution DNA melting analysis: Advancements and limitations. Hum Mutat. 2009;30(6):857–9. doi: 10.1002/humu.20951.
23. Tong SYC, Giffard PM. Microbiological applications of high-resolution melting analysis. J Clin Microbiol. 2012;50(11):3418–21. doi: 10.1128/JCM.01709-12.
24. Lipsky RH, Mazzanti CM, Rudolph JG, Xu K, Vyas G, Bozak D, et al. DNA Melting Analysis for Detection of Single Nucleotide Polymorphisms. Clin Chem . 2001;47(4):635–44. doi: 10.1093/clinchem/47.4.635.
25. Elenitoba-Johnson KSJ, Bohling SD. Solution-Based Scanning for Single-Base Alterations Using a Double-Stranded DNA Binding Dye and Fluorescence-Melting Profiles. Am J Pathol . 2001;159(3):845–53. doi: 10.1016/S0002-9440(10)61760-9.
26. Gundry CN, Vandersteen JG, Reed GH, Pryor RJ, Chen J, Wittwer CT. Amplicon Melting Analysis with Labeled Primers: A Closed-Tube Method for Differentiating Homozygotes and Heterozygotes. Clin Chem . 2003;49(3):396–406. doi: 10.1373/49.3.396.
27. Vandersteen JG, Bayrak-Toydemir P, Palais RA, Wittwer CT. Identifying common genetic variants by high-resolution melting. Clin Chem. 2007;53(7):1191–8. doi: 10.1373/clinchem.2007.085407.
28. Li M, Palais RA, Zhou L, Wittwer CT. Quantifying variant differences in DNA melting curves: Effects of length, melting rate, and curve overlay. Anal Biochem. 2017;539:90–5. doi: 10.1016/j.ab.2017.10.015.
29. Kockum I, Huang J, Stridh P. Overview of Genotyping Technologies and Methods. Curr Protoc. 2023;3(4). doi: 10.1002/cpz1.727.

30. Untergasser A, Cutcutache I, Koressaar T, Ye J, Faircloth BC, Remm M, et al. Primer3-new capabilities and interfaces. Nucleic Acids Res. 2012;40(15). doi: 10.1093/nar/gks596.
31. Okonechnikov K, Golosova O, Fursov M, Varlamov A, Vaskin Y, Efremov I, et al. Unipro UGENE: A unified bioinformatics toolkit. Bioinformatics. 2012;28(8):1166–7. doi: 10.1093/bioinformatics/bts091.
32. Liew M, Pryor R, Palais R, Meadows C, Erali M, Lyon E, et al. Genotyping of single-nucleotide polymorphisms by high-resolution melting of small amplicons. Clin Chem. 2004;50(7):1156–64. doi: 10.1373/clinchem.2004.032136.
33. Orita M, Iwahana H, Kanazawat H, Hayashi K, Sekiya T. Detection of polymorphisms of human DNA by gel electrophoresis as single-strand conformation polymorphisms (mobility shift of separated strands/point mutation/riction franment length polymorphism). Proc. Natd. Acad. Sci. 1989;86(8):2766-70. doi: 10.1073/pnas.86.8.2766.
34. Highsmith WE, Jin Q, Nataraj AJ, O'Connor JM, Burland VD, Baubonis WR, et al. Use of a DNA toolbox for the characterization of mutation scanning methods. I: Construction of the toolbox and evaluation of heteroduplex analysis. Electrophoresis. 1999;20(6):1186–94. doi: 10.1002/(SICI)1522-2683(19990101)20:6<1186::AID-ELPS1186>3.0.CO;2-6.
35. Li Q, Liu Z, Monroe H, Culiat CT. Integrated platform for detection of DNA sequence variants using capillary array electrophoresis. Electrophoresis. 2002;23(10):1499–511. doi: 10.1002/1522-2683(200205)23:10<1499::AID-ELPS1499>3.0.CO;2-X.
36. Xiao W, Oefner PJ. Denaturing high-performance liquid chromatography: A review. Hum Mutat. 2001;17(6):439–74. doi: 10.1002/humu.1130.
37. Reed GH, Wittwer CT. Sensitivity and specificity of single-nucleotide polymorphism scanning by high-resolution melting analysis. Clin Chem. 2004;50(10):1748–54. doi: 10.1373/clinchem.2003.029751.
38. Li BS, Wang XY, Ma FL, Jiang B, Song XX, Xu AG. Is High Resolution Melting Analysis (HRMA) accurate for detection of human disease-associated mutations? A meta analysis. PLoS One. 2011;6(12). doi: 10.1371/journal.pone.0028078.
39. Fitarelli-Kiehl M, Macedo GS, Schlatter RP, Koehler-Santos P, Da Silveira Matte U, Ashton-Prolla P, et al. Comparison of multiple genotyping methods for the identification of the cancer predisposing founder mutation p.R337H in TP53. Genet Mol Biol. 2016;39(2):203–9. doi: 10.1590/1678-4685-GMB-2014-0351.
40. Erali M, Voelkerding K V., Wittwer CT. High resolution melting applications for clinical laboratory medicine. Exp Mol Pathol. 2008;85(1):50–8. doi: 10.1016/j.yexmp.2008.03.012.
41. Gundry CN, Dobrowolski SF, Martin YR, Robbins TC, Nay LM, Boyd N, et al. Base-pair neutral homozygotes can be discriminated by calibrated high-resolution melting of small amplicons. Nucleic Acids Res. 2008;36(10):3401–8. doi: 10.1093/nar/gkn204.
42. Vossen RHAM, Aten E, Roos A, Den Dunnen JT. High-resolution melting analysis (HRMA) - More than just sequence variant screening. Hum Mutat. 2009;30(6):860–6. doi: 10.1002/humu.21019.
43. Li M, Zhou L, Palais RA, Wittwer CT. Genotyping accuracy of high-resolution DNA melting instruments. Clin Chem. 2014;60(6):864–72. doi: 10.1373/clinchem.2013.220160.
44. Montgomery J, Wittwer CT, Kent JO, Zhou L. Scanning the cystic fibrosis transmembrane conductance regulator gene using high-resolution DNA melting analysis. Clin Chem. 2007;53(11):1891–8. doi: 10.1373/clinchem.2007.092361.
45. Martino A, Mancuso T, Rossi AM. Application of high-resolution melting to large-scale, high-throughput SNP genotyping: A comparison with the TaqMan® method. J Biomol Screen. 2010;15(6):623–9. doi: 10.1177/1087057110365900.
46. Słomka M, Sobalska-Kwapis M, Wachulec M, Bartosz G, Strapagiel D. High resolution melting (HRM) for high-throughput genotyping-limitations and caveats in practical case studies. Int J Mol Sci. 2017;18(11):2316. doi: 10.3390/ijms18112316.
47. Aswathy N, P R, TMA S, V V, C Y, M P. Advancing livestock and poultry disease diagnosis with high-resolution melt curve analysis. International Journal of Veterinary Science and Research. 2024;10(2):021–8. doi: 10.17352/ijvsr.000146.
48. Reed GH, Wittwer CT. Sensitivity and specificity of single-nucleotide polymorphism scanning by high-resolution melting analysis. Clin Chem. 2004;50(10):1748–54. doi: 10.1373/clinchem.2003.029751.
49. Tong SYC, Lilliebridge RA, Holt DC, McDonald MI, Currie BJ, Giffard PM. High-resolution melting analysis of the spa locus reveals significant diversity within sequence type 93 methicillin-resistant Staphylococcus aureus from northern Australia. Clinical Microbiology and Infection. 2009;15(12):1126–31. doi: 10.1111/j.1469-0691.2009.02732.x.
50. Keikha M, Karbalaei M. High resolution melting assay as a reliable method for diagnosing drug-resistant TB cases: a systematic review and meta-analysis. BMC Infect Dis. 2021;21(1):989. doi: 10.1186/s12879-021-06708-1.